

# Effect of boron addition on fluorine doped ZnO particles

S. Kerli<sup>1\*</sup>, U. Alver<sup>1,2</sup>, H. Yaykaşlı<sup>1</sup>, M. Okumuş<sup>3</sup>

<sup>1</sup>*Kahramanmaraş Sutcu Imam University, Department of Physics, 46100 Kahramanmaraş, Turkey*

<sup>2</sup>*International University of Sarajevo, Department of Electrical and Electronics Engineering,  
71210 Sarajevo, Bosnia and Herzegovina*

<sup>3</sup>*Batman University, Department of Metallurgical and Materials Engineering, 72100 Batman, Turkey*

Received 19 August 2013, received in revised form 11 October 2013, accepted 26 November 2013

## Abstract

ZnO particles co-doped with boron and fluorine (B, F-ZnO) were prepared by a simple hydrothermal technique. The reaction took place in an autoclave at 200 °C for 4 h. Then the particles were annealed at 600 °C for 1 h and the characteristics of the particles were investigated as a function of boron (1, 3 and 5 at.%) and fluorine (3 at.%) concentrations in the solution. X-ray diffraction (XRD) measurements showed that doped ZnO particles had hexagonal wurtzite structure for all precursor solutions. Morphological characterization of the particles was done by a scanning electron microscope (SEM) and the results showed that the morphologies of all doped particles had a regular hexagonal shape. Thermal properties of particles were investigated by TG-DTA analysis. The optical measurements reveal that all absorption curves exhibit an observable absorption in the range 320–400 nm, with the absorption edge in between 380 and 375 nm.

**Key words:** ZnO particles, hydrothermal method, physical properties, optical properties

## 1. Introduction

Zinc oxide (ZnO), a wide bandgap semiconductor material with an energy gap of 3.37 eV and large excitation binding energy (60 meV), has attracted a great deal attention for its potential applications including surface acoustic wave filters, chemical sensors, transparent conductor, light-emitting diodes, solar cells, and optical modulator wave-guides, etc. [1–5]. Various synthesis methods have been used to grow these devices based on ZnO films. These methods include thermal evaporation, chemical vapor deposition, sol-gel method, electrochemical deposition, ion beam assisted deposition, rf magnetron sputtering deposition, spray pyrolysis and hydrothermal deposition. Among them, hydrothermal synthesis is the most attractive especially due to the fact that it allows perfect control of purity, crystallinity, composition, size and morphology by simple tuning of the experimental variables: the reaction temperature, the time, the reactant molar ratio and/or addition of the appropriate capping agents. Moreover, hydrothermal synthesis is en-

vironmentally safe and economical for large-scale production [6–10]. In recent years, introducing cation and anion impurities in ZnO structure offer an effective approach to adjust structural, optical and electrical properties [11–15].

In literature, although there are a few papers related with both B and F doped ZnO films prepared with electrospraying and room temperature spraying method [16, 17], we could not encounter any work related with B and F doped ZnO particles. For instance, Mahmood et al. [16] investigated the structural, morphological, optical and electrical properties of ZnO films while keeping B concentration fixed at 2 at.% and changing F concentration from 0–10 at.%. Similarly, Kim et al. [17] worked on optical and electrical properties of ZnO thin film by changing F concentration while keeping the B concentration fixed. In this paper, different from literature studies, we studied the boron and fluorine doped ZnO particles by keeping F concentration fixed as 3 at.% and changing B concentration as 1, 3, and 5 at.%. We also investigated the structural, morphological and optical properties

\*Corresponding author: tel.: +90 344 219 1487; fax: +90 344 219 1042; e-mail address: [suleymankerli@yahoo.com](mailto:suleymankerli@yahoo.com)

of boron and fluorine doped ZnO particles.

## 2. Experimental details

The precursor solution was prepared by dissolving 0.1 M of zinc chloride ( $\text{ZnCl}_2$ ), 0.1 M of hexamethylenetetramine (HMT,  $\text{C}_6\text{H}_{12}\text{N}_4$ ), 0.1 M of ammonium fluoride ( $\text{NH}_4\text{F}$ ), and 0.1 M of boric acid ( $\text{H}_3\text{BO}_3$ ) in 100 ml deionized water. The fluorine concentrations in precursor solutions were adjusted in terms of atomic percentage 3 %, boron concentrations (1, 3 and 5 at.%) with respect to zinc. Hydrothermal growth was carried out at 200 °C in an autoclave placed in a furnace for 4 h. After cooling naturally to room temperature, the transparent supernatant was removed by pipette and white ZnO precipitate was lifted out. The obtained particles were washed with distilled water several times and dried at room temperature in air for further characterization. All experimental conditions were kept the same for all samples. To investigate the effect of annealing, the particles were annealed at 600 °C for 1 h in air.

The crystal structures of ZnO particles were investigated by Philips X'Pert Pro X-ray diffractometer (XRD), with  $\text{Cu K}\alpha$  radiation, the surface morphologies were observed using a Zeiss EVO-LS10 scanning electron microscopy (SEM) images. Thermal gravimetric and differential thermal analysis (TG-DTA) curves were conducted with a Perkin-Elmer Diamond TG-DTA at a heating rate of 40 °C  $\text{min}^{-1}$  in air. Optical properties of samples were obtained by using a Shimadzu UV-1800 ultraviolet-visible spectrometer (UV-vis).

## 3. Results and discussion

XRD pattern of fluorine and boron-doped ZnO particles, produced by hydrothermal method, are shown in Fig. 1a,b. Spectra can be indexed to hexagonal wurtzite-type ZnO crystal structures consistent with the values in the standard card (PDF-2, reference code: 00-036-1451).

As seen in Fig. 1a,b, the contribution of fluorine and boron does not change the hexagonal wurtzite structure. It is clearly seen that with the contribution of fluorine, peak intensity of ZnO particles decreases. Moreover, introducing boron impurities to ZnO structure also causes the decrease of the peak intensities of ZnO particles. From Fig. 1a, some small intense peaks between (100) and (200) peaks are also observed. It is considered that these small peaks are originated from hydroxide compounds of Zn. As seen clearly in Fig. 1b, when the particles are annealed at 600 °C for 1 h, these small impurity peaks are completely removed from XRD pattern of particles. In addition, for annealed

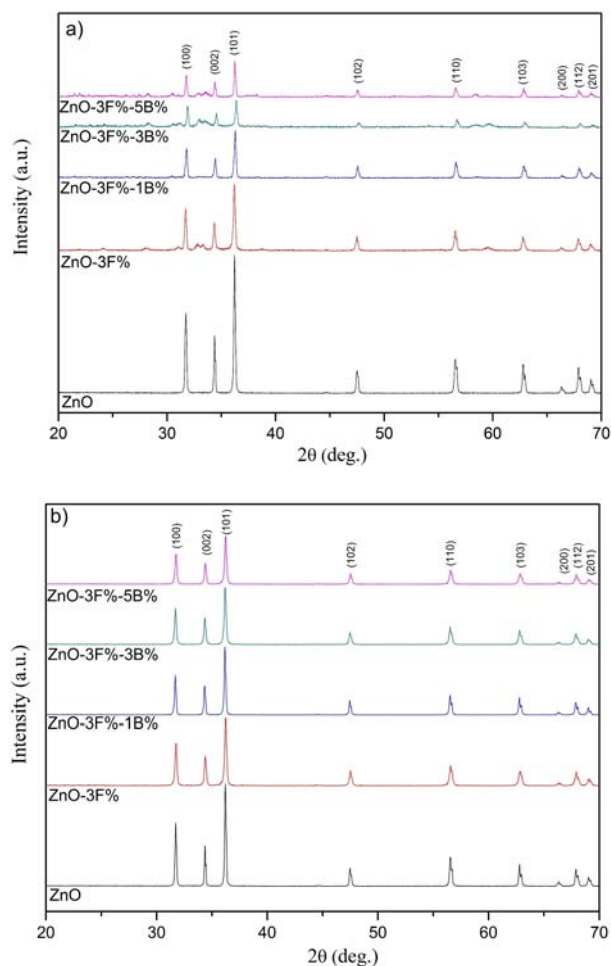


Fig. 1. XRD spectra of (a) as prepared and (b) annealed B:F-ZnO particles.

samples (Fig. 1b), the peak intensities of the planes are also found to decrease with fluorine and increase boron doping concentration for all samples. This indicates that the crystalline quality of the B:F-ZnO particles degrades when the fluorine and boron doping increases. The reason for that might be the crystal distortion by substitution of lower ionic radius fluorine (133 pm) and boron (0.027 nm), which hinder the growth of ZnO peaks. In addition, gradual change in peak intensity implies that F and B atoms substitute for Zn atoms in the structure.

The chemical structure of ZnO doped with low percentages fluorine 3 at.% and (0.1, 3 and 5 at.%) of boron was controlled by FTIR spectra. But due to the low rate of contribution of boron and fluorine, we could not observe any peak associated with phases of boron and fluorine atoms in FTIR spectra. Similarly, the EDX analysis was performed, but the rates of the particles in the determination of fluorine and boron were also inadequate.

TG-DTA curves of ZnO and 3 % of fluorine-3 at.% of boron doped ZnO particles are shown in Fig. 2a,b.

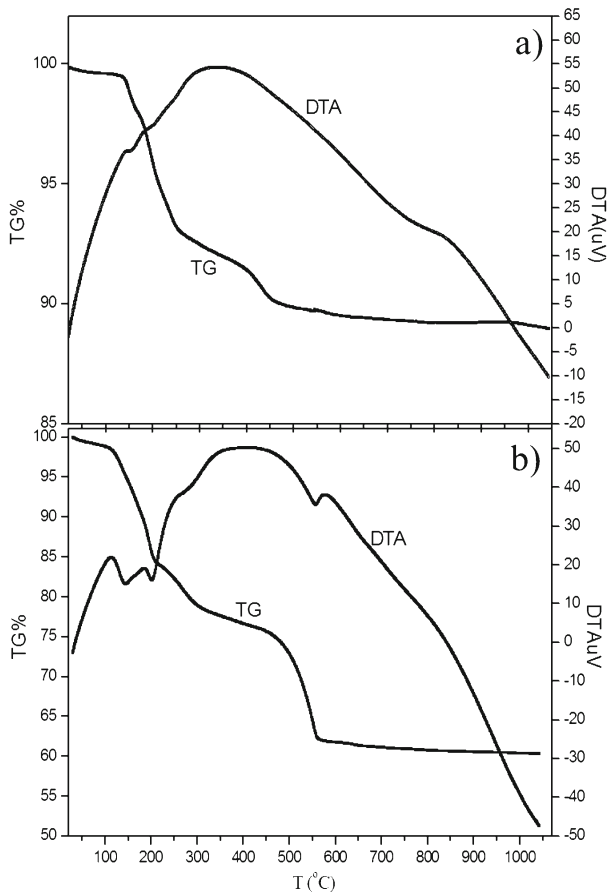
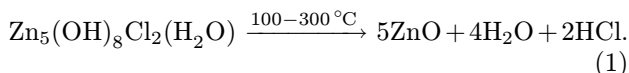


Fig. 2. TG-DTA trace for (a) ZnO particles, (b) 3 % fluorine and 3 % boron doped ZnO particles.

In Fig. 2a, the TG curve shows two step weight losses. The first step at around 100–300 °C corresponds to the loss of water molecules on the surface and inter-layer of the ZnO particles. The second step occurs at 300–600 °C due to the decomposition of hydroxide and other compounds in the precursor solutions. As seen in Fig. 2a, the total weight loss is about 11 % for the ZnO particles. For the Zn's hydroxide compounds structure, the first weight loss occurred at a temperature of between 100 and 300 °C, which corresponded to the loss of water molecules from  $Zn_5(OH)_8Cl_2H_2O$ , to form ZnO and zinc chloride and hydrochloric acid [18]:



The second weight loss occurred at a temperature of between 300 and 600 °C, which was attributed to the conversion of  $Zn_5(OH)_8Cl_2H_2O$  to complete zinc oxide [19]. TG-DTA curves of %3F – %3B doped ZnO particles are shown in Fig. 2b. Similarly, mass loss recorded at low temperature was due to evaporation of the solvent. The total weight loss was about 39 % for the particles. The loss of mass of the structure is

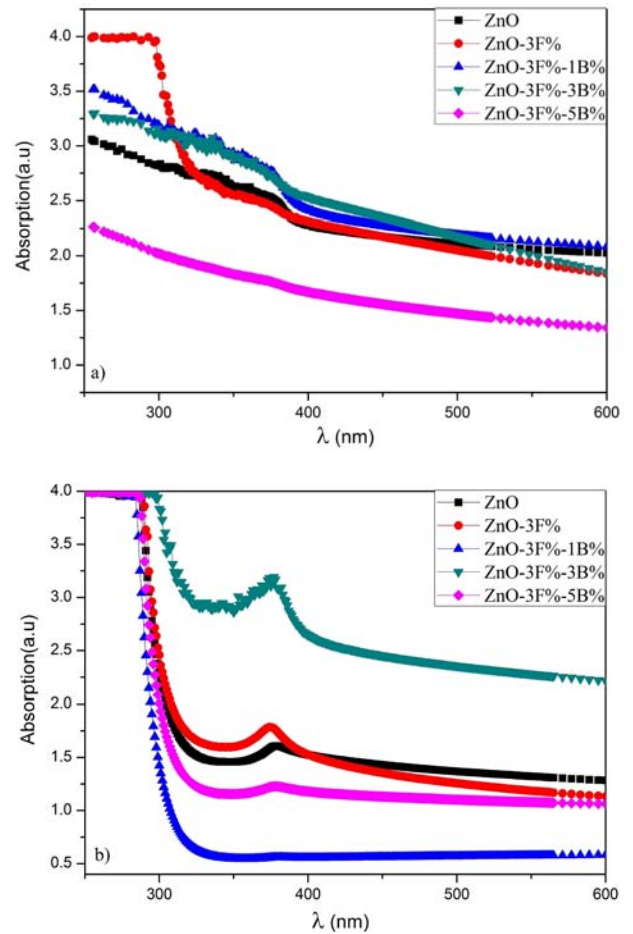


Fig. 3. Absorption spectra of B doped F-ZnO particles: (a) as deposited, (b) annealed.

thought to be a result of evaporation of organics at 600 °C [18, 20].

Figure 3a,b shows annealed and as deposited UV-visible absorbance spectra of B doped F-ZnO particles. As seen in Fig. 3a, all absorption curves exhibit an observable absorption in the range 320–400 nm, with the absorption edge in between 380 and 375 nm, due to the large excitation binding energy. As seen clearly in Fig. 3b, sharpness of the peaks of maximum absorption increases after annealing due to divergence of organic and hydroxide. This supports that the crystal structure is better after annealing. In addition, from Fig. 3 it can be seen that the absorbance edge decreases with increasing boron concentration for all samples. The shift of absorbance edge to the shorter wavelength (higher band gap) is the Burstein-Moss effect [21], which is due to the increase of carrier concentration.

SEM images of as deposited and annealed boron doped F-ZnO particles obtained with hydrothermal method are shown in Figs. 4 and 5, respectively. As seen in these figures, the distribution, size and micro-

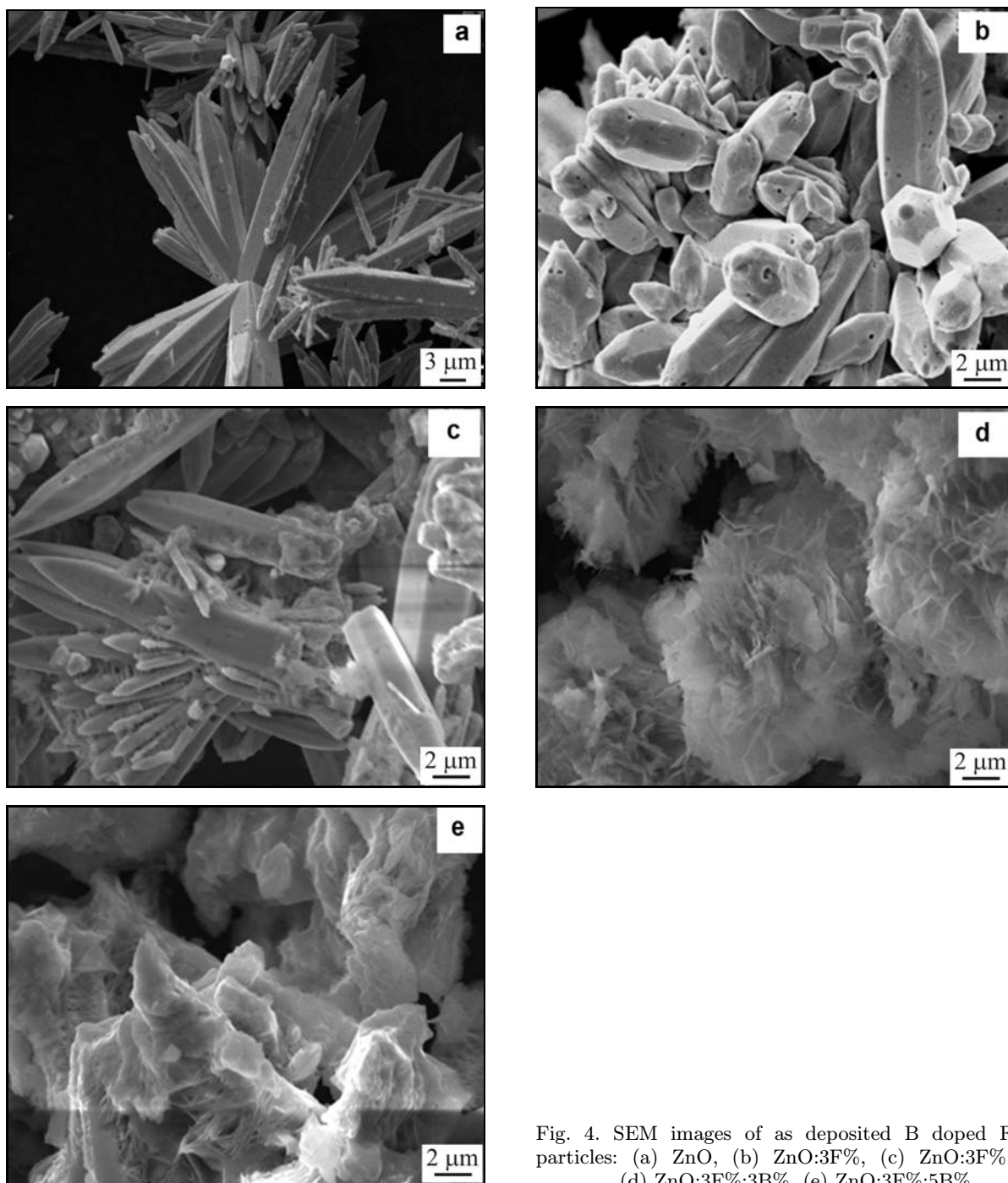


Fig. 4. SEM images of as deposited B doped F-ZnO particles: (a) ZnO, (b) ZnO:3F%, (c) ZnO:3F%:1B%, (d) ZnO:3F%:3B%, (e) ZnO:3F%:5B%.

structure of the ZnO powders change with the boron and fluorine doping concentration significantly for all samples. From SEM images, for as deposited samples (Fig. 4), it was observed that when B concentration increased in the solution, hexagonal rod structure became deformed and turned into rose-like structure. This rose-like structure should be originated due to hydroxide component of Zn. These results are in agreement with the XRD results. For annealed samples (Fig. 5), it is seen that the rose-like structure assigned to hydroxide compounds disappears and the length of

rod particles is decreasing with increasing boron concentration in structure.

#### 4. Conclusions

In this study, undoped and boron doped F-ZnO particles were produced by hydrothermal method. XRD and SEM analyses have confirmed that the microcrystals have a crystalline structure with pure wurtzite-type crystallites. Particles annealed at 600 °C



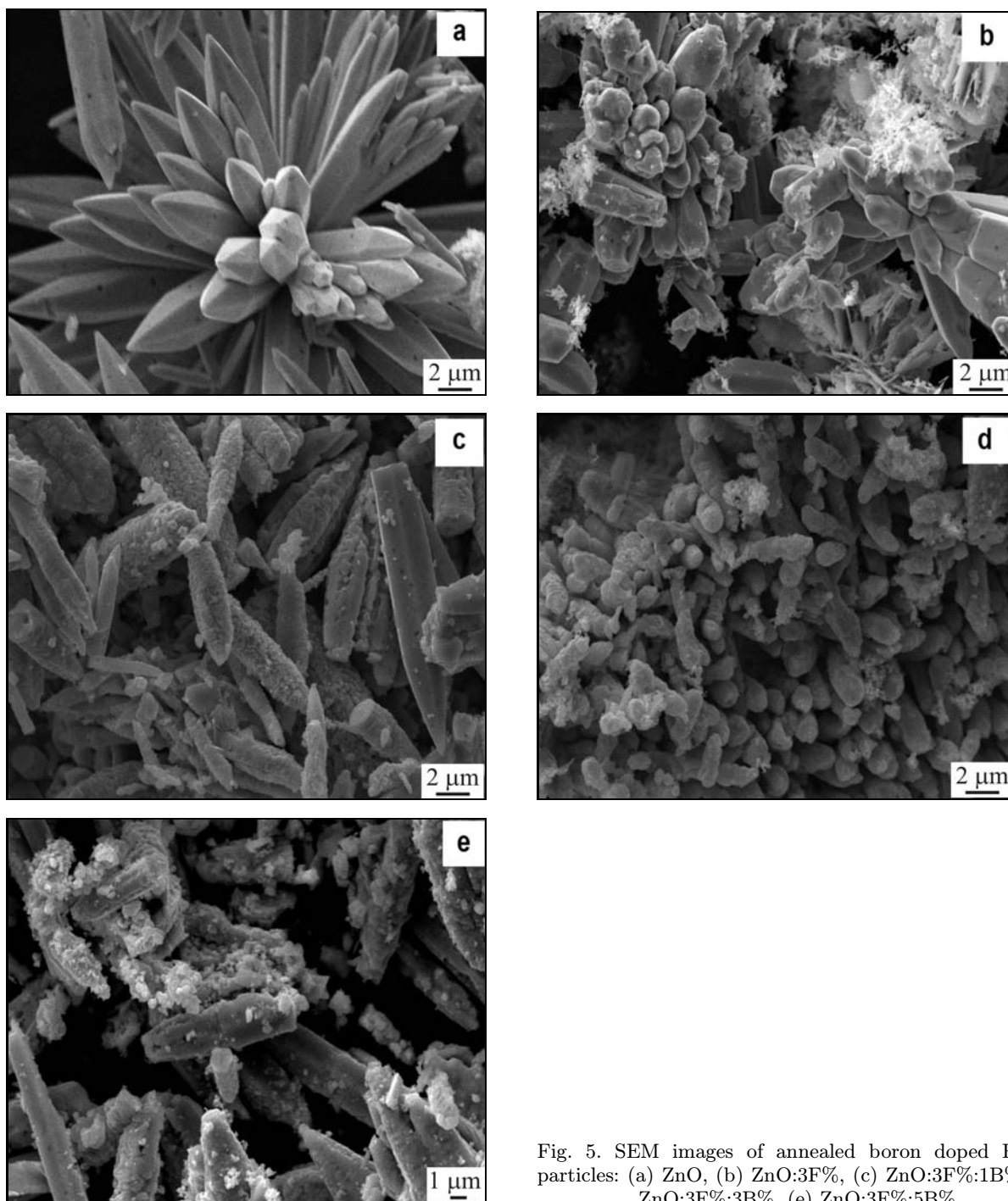


Fig. 5. SEM images of annealed boron doped F-ZnO particles: (a) ZnO, (b) ZnO:3F%, (c) ZnO:3F%:1B%, (d) ZnO:3F%:3B%, (e) ZnO:3F%:5B%.

were found to have a better structure. Thermal gravimetric measurements show that thermal decomposition of hydroxide compounds of Zn atoms is occurred at 600°C. From UV-Vis spectrum, we find that absorption edges of ZnO powders are decreasing with increasing boron concentration. It is observed that morphologies of ZnO particles are influenced by the addition of boron impurity and the size of fluorine doped ZnO particles reduced with increasing concentration.

## References

- [1] Kong, Y. C., Yu, D. P., Zhang, B., Fang, W., Feng, S. Q.: *Appl. Phys. Lett.*, 78, 2001, p. 407. [doi:10.1063/1.1342050](https://doi.org/10.1063/1.1342050)
- [2] Yang, P. D., Yan, H. Q., Mao, S., Russo, R., Johnson, J., Saykally, R., Morris, N., Pham, J., He, R. R., Choi, H.-J.: *Adv. Funct. Mater.*, 12, 2002, p. 323. [doi:10.1002/1616-3028\(20020517\)12:5<323::AID-ADFM323>3.0.CO;2-G](https://doi.org/10.1002/1616-3028(20020517)12:5<323::AID-ADFM323>3.0.CO;2-G)
- [3] Lamb, D. A., Irvine, S. J. C.: *J. Cryst. Growth*, 273,

- 2004, p. 111. [doi:10.1016/j.jcrvsgro.2004.08.027](https://doi.org/10.1016/j.jcrvsgro.2004.08.027)
- [4] Look, D. C.: *Mater. Sci. Eng. B.*, *80*, 2001, p. 383. [doi:10.1016/S0921-5107\(00\)00604-8](https://doi.org/10.1016/S0921-5107(00)00604-8)
- [5] Hara, K., Horiguchi, T., Kinoshita, T., Sayama K., Sugihara, H., Arakawa, H.: *Sol. Energ. Mater. Sol. C*, *64*, 2000, p. 115. [doi:10.1016/S0927-0248\(00\)00065-9](https://doi.org/10.1016/S0927-0248(00)00065-9)
- [6] Lu, C.-H., Yeh, C.-H.: *Ceramics International*, *26*, 2000, p. 351. [doi:10.1016/S0272-8842\(99\)00063-2](https://doi.org/10.1016/S0272-8842(99)00063-2)
- [7] Wang, Y., Li, X., Lu, G., Chen, G., Chen, Y.: *Materials Letters*, *62*, 2008, p. 2359. [doi:10.1016/j.matlet.2007.12.019](https://doi.org/10.1016/j.matlet.2007.12.019)
- [8] Zhang, Y., Mu, J.: *Nanotechnology*, *18*, 2007, 075605, 6 pp.
- [9] Yi, R., Zhang, N., Zhou, H., Shi, R., Qiu, G., Liu, X.: *Materials Science and Engineering B*, *153*, 2008, p. 25. [doi:10.1016/j.mseb.2008.09.017](https://doi.org/10.1016/j.mseb.2008.09.017)
- [10] Cavalcante, L. S., Sczancoski, J. C., Siu Li, M., Longo, E., Varela, J. A.: *Colloids and Surfaces A: Physicochemical and Engineering Aspects*, *396*, 2012, p. 346. [doi:10.1016/j.colsurfa.2011.12.021](https://doi.org/10.1016/j.colsurfa.2011.12.021)
- [11] Bacaksiz, E., Aksu, S., Yilmaz, S., Parlak, M., Altunbaş, M.: *Thin Solid Films*, *518*, 2010, p. 4076. [doi:10.1016/j.tsf.2009.10.141](https://doi.org/10.1016/j.tsf.2009.10.141)
- [12] Huang, S., Xiao, Q., Zhou, H., Wang, D., Jiang, W.: *J. Alloy Compd.*, *486*, 2009, p. L24. [doi:10.1016/j.jallcom.2009.07.033](https://doi.org/10.1016/j.jallcom.2009.07.033)
- [13] Wang, Y. S., John Thomas, P., O'Brien, P.: *J. Phys. Chem. B*, *110*, 2006, p. 21412. [doi:10.1021/jp0654415](https://doi.org/10.1021/jp0654415)
- [14] Lokhande, B. J., Patil, P. S., Uplane, M. D.: *Physica B*, *302–303*, 2001, p. 59. [doi:10.1016/S0921-4526\(01\)00405-7](https://doi.org/10.1016/S0921-4526(01)00405-7)
- [15] Al-Harbi, T.: *J. Alloy Compd.*, *509*, 2011, p. 387. [doi:10.1016/j.jallcom.2010.09.034](https://doi.org/10.1016/j.jallcom.2010.09.034)
- [16] Khalid Mahmood, Seung Bin Park: *J. Cryst. Growth*, *361*, 2012, p. 30. [doi:10.1016/j.jcrvsgro.2012.08.018](https://doi.org/10.1016/j.jcrvsgro.2012.08.018)
- [17] Gil Ho Kim, Deok Hyun Hwang, Seong Ihl Woo: *Material. Chem. Phys.*, *131*, 2011, p. 77. [doi:10.1016/j.matchemphys.2011.07.055](https://doi.org/10.1016/j.matchemphys.2011.07.055)
- [18] Long, T., Yin, S., Takabatake, K., Zhnag, P., Sato, T.: *Nanoscale Res. Lett.*, *4*, 2009, p. 247. [doi:10.1007/s11671-008-9233-2](https://doi.org/10.1007/s11671-008-9233-2)
- [19] Kerli, S.: Fabrication and physical properties of bor-fluorine doped ZnO particles and thin films (Phd Thesis). Kahramanmaras, Kahramanmaras Sutcu Imam University 2012.
- [20] Yin, S., Goto, T., Gobo, F., Huang, Y. F., Zhang, P. L., Sato, T.: *IOP Conference Series: Materials Science and Engineering*, *18*, 2004, p. 42004. [doi:10.1088/1757-899X/18/4/042004](https://doi.org/10.1088/1757-899X/18/4/042004)
- [21] Burnstein, E.: *Phys. Rev.*, *93*, 1954, p. 632. [doi:10.1103/PhysRev.93.632](https://doi.org/10.1103/PhysRev.93.632)